Chiral and nonorthogonal eigenstate pairs in open quantum systems with weak backscattering between counterpropagating traveling waves

Jan Wiersig
Institut für Theoretische Physik, Universität Magdeburg, Postfach 4120, D-39016 Magdeburg, Germany
(Received 1 October 2013; published 22 January 2014)

We study the properties of energy eigenstates in open quantum systems in which clockwise and counterclockwise traveling waves are weakly coupled. We show that under rather general conditions the energy eigenstates of such systems can appear in pairs of nonorthogonal, copropagating traveling-wave states. The relation to exceptional points of the effective non-Hermitian Hamiltonian is discussed.

DOI: 10.1103/PhysRevA.89.012119 PACS number(s): 03.65.−w, 42.25.Bs, 03.65.Nk

I. INTRODUCTION

The physics of open quantum and wave systems plays an important role in several research areas. Examples are ultracold atoms and molecules in optical lattices [1,2], semiconductor quantum dots coupled to phonons [3], parity-time symmetric systems in optics [4], microwave systems [5,6], and optical microcavities [7]. The most obvious aspect of the coupling to an environment is that it can convert bound energy eigenstates into decaying quasibound states as already introduced by Gamow [8] in 1928.

In the case of optical microcavities the decay stems from optical losses due to absorption and radiation. Deformed optical microdisks are in particular interesting cavities to study quantum chaos [9–11] and nontrivial consequences of the openness [12,13] both in theory and experiment. Recently, it has been discovered in numerical simulations that the coherent backscattering of counterpropagating waves in such deformed cavities can be asymmetric provided that the cavity does not possess a mirror-reflection symmetry [12,14]. This asymmetric backscattering has counterintuitive consequences, such as the appearance of pairs of optical modes (the analog of quasibound states), where in each pair (i) the two modes are significantly nonorthogonal, (ii) each of the two modes has a finite orbital angular momentum ("chirality") and (iii) both modes mainly copropagate in the same direction. This nonorthogonality, chirality, and copropagation is strongly enhanced near so-called exceptional points (EPs; see [15–17]) in parameter space at which two or more eigenvalues *and* eigenstates coalesce. This above-mentioned chirality is related to the intrinsic chirality of EPs [18,19] and not to optical activity in chiral media; see, e.g., [20]. The asymmetric backscattering and the resulting nonorthogonality and chirality is not limited to deformed microdisk cavities. It also shows up in microdisks perturbed by small external scatterers [21] and in parity-time-symmetric quantum rings [22].

The aim of this paper is to reveal that this set of interrelated phenomena arise generically in all quantum and linear wave systems provided the following conditions are simultaneously met: (i) the system is open, (ii) no mirror-reflection symmetries are present, and (iii) backscattering between counterpropagating waves is weak. Our analysis is restricted to time-reversal-symmetric systems which can be described, at least in a local sense, by an effective non-Hermitian Hamiltonian [23]. Such effective Hamiltonians have been routinely and successfully applied to various physical systems, e.g., microwave cavities [24], in the context of the complex-scaling method for the study of atomic and molecular dynamics [25], ultracold atoms in optical lattices [1,26], quantum-dot-microcavity systems [27], in nuclear physics [28], and to electron transport in low-dimensional nanostructures [29].

This article is organized as follows: Section II provides a simple physical system to demonstrate the relevant effects. In Sec. III, the general theory is formulated. Finally, some concluding remarks are given in Sec. IV.

II. ILLUSTRATIVE EXAMPLE

To illustrate the phenomenology of the "troika" consisting of nonorthogonality, chirality, and copropagation we analyze the simplest possible example, which is a single quantum particle of mass M moving along a circle in a complex potential. Using a normalized coordinate $x \in [0,2\pi)$ and energy units such that $\hbar^2/2M = 1$, the effective Hamiltonian reads in coordinate representation

$$H_{\text{eff}} = -\frac{\partial^2}{\partial x^2} + V(x). \tag{1}$$

We consider the linear potential

$$V(x) = V_0 x, \tag{2}$$

which does not possess any mirror-reflection symmetry unless $V_0 = 0$. With the coordinate x unfolded to the real axis, $V(x)$ would be a sawtooth-shaped periodic potential. A sawtoothlike potential with real V_0 has been realized in antidot arrays [30] and for ultracold atoms in optical lattices [31]. For the latter type of systems it is also possible to design complex optical potentials, the (negative) imaginary part of which describes an incoherent loss of atoms, in a controlled manner [1]. So, the case of complex V_0, for which the Hamiltonian (1) is non-Hermitian, might be realized in this type of systems. Note that the Hamiltonian (1) obeys time-reversal symmetry also for complex potentials, in the sense that time reversal maps decaying states into states which increase in time and vice versa [32].

In the trivial situation $V_0 = 0$ the eigenstates of the Hamiltonian (1) can be written as

$$\Phi_m(x) = \frac{1}{\sqrt{2\pi}} \exp(imx) \tag{3}$$

with quantum number $m \in \mathbb{Z}$. Since the configuration space has the topology of a circle, m plays the role of an orbital

angular momentum number. Positive m correspond to counterclockwise (CCW) traveling waves, negative m to clockwise (CW) traveling waves. The energy eigenvalues m^2 are twofold degenerate for $|m| \neq 0$, so the eigenstates with the same $|m|$ can be superimposed to give new eigenstates, e.g., standing waves $\cos mx$ and $\sin mx$ with $m = 1,2,\ldots$.

For real $V_0 \neq 0$, exact solutions for the energy eigenstates have been derived in Ref. [33] in terms of Airy functions. However, the resultant transcendental equations are not helpful for our purpose. We therefore rely on a full numerical solution of the eigenvalue problem for the complex potential. To determine the numerical solution, the right eigenstates $\psi_j(x)$ of the Hamiltonian (1) are expanded in the angular momentum basis

$$\psi_j(x) = \sum_{m=-\infty}^{\infty} \alpha_{j,m} \Phi_m(x). \tag{4}$$

The Hamiltonian H_{eff} is expressed as

$$H_{\text{eff}\,m,m'} = \begin{cases} m^2 + \pi V_0 & \text{if } m = m', \\ \frac{iV_0}{m-m'} & \text{otherwise.} \end{cases} \tag{5}$$

To obtain the eigenvalues $E_j \in \mathbb{C}$ and the right eigenvectors $\vec{\alpha}_j = (\alpha_{j,1}, \alpha_{j,2}, \ldots)$ of this non-Hermitian matrix we restrict the indices $|m|, |m'|$ to $m_{\max} = 1000$ and diagonalize the truncated matrix numerically.

For the following discussion we consider a complex V_0 with $\text{Im}(V_0) < 0$ describing absorption. The case of amplification, $\text{Im}(V_0) > 0$, can be deduced from time reversal. We choose $V_0 = 1 - i$ without loss of generality. Figure 1 shows the complex eigenvalues E_j of the first 45 states ordered according to increasing real part of E_j. The imaginary part of E_j is the decay rate of the jth state. It can be clearly seen that the twofold degeneracy is broken, but for not too small energies the eigenvalues appear in nearly degenerate pairs. This can be easily understood as for not too small $|m|$ the absolute value of the potential $V(x)$ is much smaller than the unperturbed

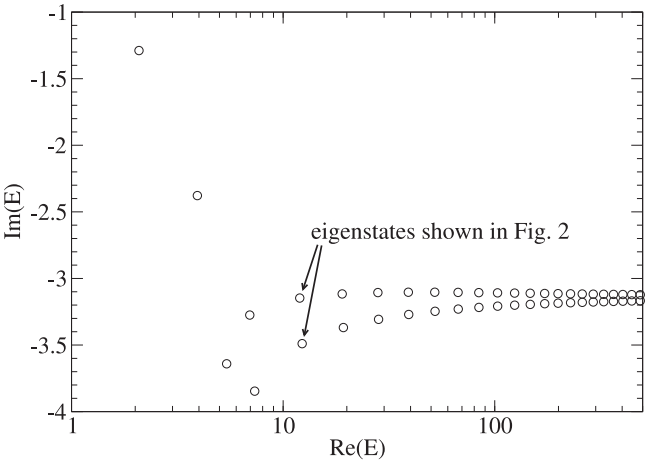

FIG. 1. Calculated complex eigenvalues E_j of the effective Hamiltonian (1) with complex potential (2) using $V_0 = 1 - i$. The splitting of the pairs is relatively strong for the first states and decreases for increasing real part of the energy. Note the logarithmic scale on the horizontal axis.

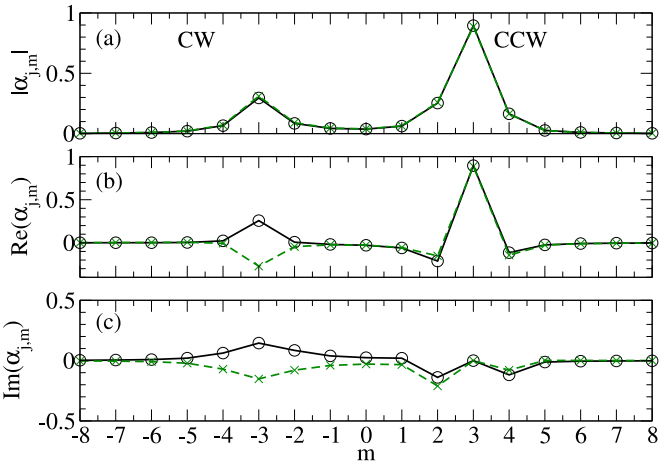

FIG. 2. (Color online) Components of the eigenvectors $\vec{\alpha}_6$ (circles and black solid lines) and $\vec{\alpha}_7$ (crosses and green dashed lines): (a) absolute value (both curves are on top of each other), (b) real, and (c) imaginary part; the phase of the eigenvectors is chosen such that $\text{Im}(\alpha_{j,3}) = 0$. The corresponding energy eigenvalues are marked in Fig. 1. The lines are guides to the eye.

part of the Hamiltonian m^2. Alternatively stated, the coupling between the unperturbed CW and CCW traveling components is weak and therefore the energy splitting is small.

Figure 2 displays as example the eigenvector pair $\vec{\alpha}_6$ and $\vec{\alpha}_7$ with eigenvalues $E_6 \approx 11.978\,24 - i3.147\,13$ and $E_7 \approx 12.300\,98 - i3.489\,54$. We observe a remarkable imbalance between the CW and CCW components. The CCW components are larger than the CW components by a factor of about 3. This is the chirality which has been discovered before in deformed or perturbed microdisks [12,14,21] and parity-time-symmetric quantum rings [22]. Hence, both states are mainly traveling waves. Moreover, they copropagate in the CCW direction. Figures 2(b) and 2(c) reveal the small difference between the components. For negative index m both the real and the imaginary part of the eigenvector components have a different sign for the two states. This allows us to superimpose the two eigenstates to form nearly pure CW or CCW quasimodes [12].

To quantify the relative weight of CW and CCW components we use the definition of the chirality of a state in the angular momentum basis [14],

$$\alpha = 1 - \frac{\min\left(\sum_{m=-\infty}^{-1} |\alpha_m|^2, \sum_{m=1}^{\infty} |\alpha_m|^2\right)}{\max\left(\sum_{m=-\infty}^{-1} |\alpha_m|^2, \sum_{m=1}^{\infty} |\alpha_m|^2\right)}, \tag{6}$$

where α_m stands for the components $\alpha_{j,m}$ of the state with number j. In the case of a standing-wave pattern with balanced distribution of CW and CCW components the chirality is $\alpha = 0$. This is the case for systems with mirror-reflection symmetry, and also for closed systems [14]. For the two eigenvectors $\vec{\alpha}_6$ and $\vec{\alpha}_7$ shown in Fig. 2 we get $\alpha \approx 0.8854$ and $\alpha \approx 0.8712$ which reflects the significant chirality of the states. Figure 3 reveals the fact that here all nearly degenerate states have a similar value of the chirality.

We remark that the chirality shown here is different from the unidirectional transport observed in quantum ratchets.

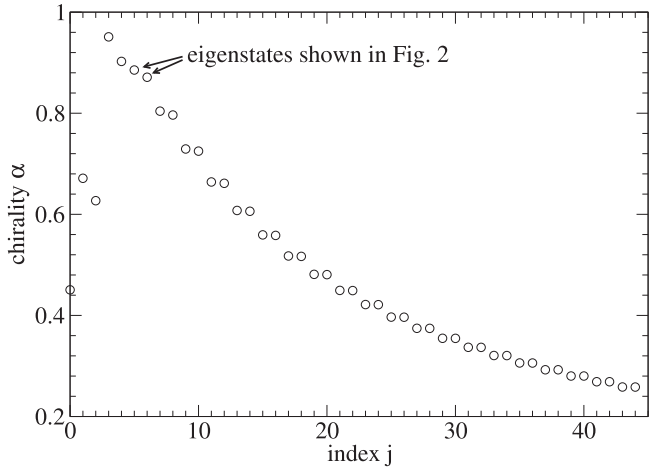

FIG. 3. Chirality α of the first 45 eigenstates vs the state index j. The two eigenstates of each nearly degenerate pair exhibit a similar chirality.

In the latter case, one or more particles initially at rest are transported by a time-dependent potential; see, e.g., [31]. For both phenomena, however, the absence of mirror-reflection symmetries is crucial.

Next, we investigate the nonorthogonality of the eigenstates. The orthogonality of two eigenstates $\psi_j(x)$ and $\psi_k(x)$ is measured by the normalized overlap integral

$$S_{jk} = \frac{\int_0^{2\pi} dx\ \psi_j^*(x)\psi_k(x)}{\sqrt{\int_0^{2\pi} dx\ \psi_j^*(x)\psi_j(x)}\sqrt{\int_0^{2\pi} dx\ \psi_k^*(x)\psi_k(x)}}. \quad (7)$$

For a given pair of eigenstates j and k we use the shorthand notation $S = |S_{jk}|$ where $0 \leqslant S \leqslant 1$. If $S = 0$ ($S = 1$) the states are orthogonal (collinear). In the presence of a mirror-reflection symmetry or for a closed system, $S_{jk} = \delta_{jk}$. For the two eigenvectors $\vec{\alpha}_6$ and $\vec{\alpha}_7$ shown in Fig. 2 the overlap turns out to be $S \approx 0.7798$, so the eigenvectors are highly nonorthogonal. Figure 4 demonstrates that such nonorthogonality can be observed also for the other pairs of nearly degenerate eigenstates. For eigenvectors which do not form a nearly degenerate pair, the nonorthogonality is typically considerably weaker. It should be mentioned that nonorthogonality of quasibound states is well known, see, e.g., [34], and plays an important role in different branches of physics, for instance it leads to excess quantum noise in open laser resonators [35–37], it influences reaction cross sections [38], and it describes the interference between long- and short-lived neutral kaon states [39].

Figure 5 summarizes the nonorthogonality and chirality of the eigenstates in our model system by showing the overlap S of each nearly degenerate eigenstate pair versus the chirality α of each state. It can be seen that the whole range from nearly orthogonal and almost no chirality to strong nonorthogonality and chirality is covered. The chirality α and overlap S are highly correlated. It fact, they fall on a curve given by the simple formula

$$\alpha = \frac{2S}{1+S}. \quad (8)$$

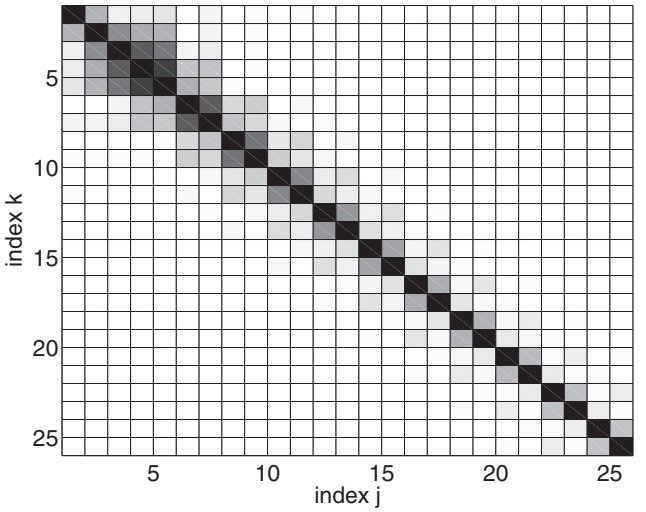

FIG. 4. The nonorthogonality matrix S_{jk} for the first 25 eigenstates. The absolute value of the matrix elements are shown as a gray-scale intensity. The maximum value 1 (corresponding to collinear vectors) is black and the minimum value 0 (orthogonal vectors) is shown in white.

This quantitative relation between chirality and nonorthogonality was concluded from a phenomenological model for deformed microdisk cavities in Ref. [14]. Figure 5 demonstrates that for our one-dimensional quantum system there is a nearly perfect agreement between the full numerical solution and Eq. (8). The next section explains why this relation works so well for this and other systems.

III. GENERAL THEORY

Having discussed a specific one-dimensional (1D) quantum system for illustration purposes in the previous section, we here show that the observed asymmetric backscattering and the resulting nonorthogonality, chirality, and copropagation is a

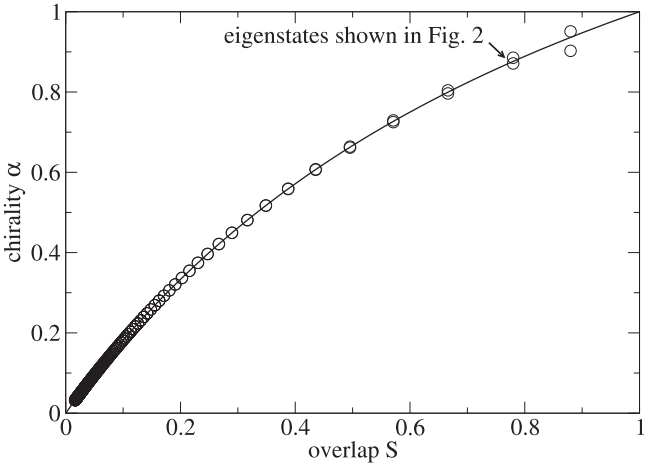

FIG. 5. Chirality α vs spatial overlap S of pairs of almost degenerate eigenstates ranging from number 4 to 400 (open circles). Results for eigenstates from 1 to 3 are not shown as they do not form unambiguous pairs; cf Fig. 1. The solid curve is given by Eq. (8).

general phenomenon appearing also in other one-dimensional as well as in two- and three-dimensional quantum or wave systems. In the following derivation we require only that (i) the system is open, (ii) no mirror-reflection symmetries are present, and (iii) backscattering between counterpropagating waves is weak.

For a 3D system we use a cylindrical coordinate system (z,r,ϕ) where the z axis is chosen to be perpendicular to the plane in which we study the backscattering of counterpropagating traveling waves. In the case of a 2D system (1D on a circle) the following formulas can be adapted by ignoring the z (and the r) coordinate. If the system has a mirror-reflection symmetry in the (r,ϕ) plane then we choose the azimuthal coordinate ϕ such that the rays $\phi = 0$ and $\phi = \pi$ are along this symmetry axis in the (r,ϕ) plane. In this coordinate system a convenient basis is given by

$$\psi_{j,c}(z,r,\phi) = \eta_j(z,r)\cos m\phi; \quad m = 0,1,2,\ldots \tag{9}$$

$$\psi_{j,s}(z,r,\phi) = \eta_j(z,r)\sin m\phi; \quad m = 1,2,\ldots, \tag{10}$$

where j comprises the three indices k, l, and m for the three degrees of freedom. We do not need to specify the functions $\eta_j(z,r)$, except that we require them to be real valued and to form an orthonormal basis.

The basis functions (9) and (10) can be considered as standing waves in the azimuthal direction. In such a basis, assuming that time-reversal invariance is not violated, a non-Hermitian Hamiltonian describing an open system is a complex-symmetric matrix. This has been shown in a general setting [32] and for systems coupled to the continuum in the framework of scattering theory [24].

For the sake of a clear discussion we consider a large but finite number of basis functions. For fixed m we use n basis functions (for 1D $n = 1$). For the azimuthal degree of freedom we use $m_{\max}$ basis functions. For short, we write $nm_{\max} = N$. In this truncated basis the effective Hamiltonian can be expressed as complex-symmetric $(2N+n)\times(2N+n)$ matrix

$$H_{\text{eff}} = \begin{pmatrix} E_0 & a & b \\ a^{\mathrm{T}} & E_c & W \\ b^{\mathrm{T}} & W^{\mathrm{T}} & E_s \end{pmatrix}. \tag{11}$$

The superscript $^{\mathrm{T}}$ denotes the transposition of a matrix. The complex-symmetric $n\times n$ matrix E_0 describes the $m = 0$ subspace. The complex-symmetric $N\times N$ matrices E_c and E_s describe the subspaces (9) (without $m = 0$) and (10), respectively. The complex $n\times N$ matrices a and b couple the $m = 0$ subspace to the subspaces (9) (without $m = 0$) and (10), respectively. The complex $N\times N$ matrix W describes the coupling between the subspaces (9) (without $m = 0$) and (10), respectively. If a mirror-reflection symmetry is present then W vanishes and there is no coupling between the two subspaces. In this case, a well-defined parity can be introduced and subspace (9) belongs to the positive parity and subspace (10) to the negative parity.

Next we employ a transformation to the traveling-wave basis

$$\tilde{\psi}_j(z,r,\phi) = \eta_j(z,r)\exp(im\phi) \tag{12}$$

with $m\in\mathbb{Z}$. This can be accomplished with the unitary $(2N+n)\times(2N+n)$ matrix

$$M^{\dagger} = \begin{pmatrix} \mathbb{1}_{n\times n} & 0 & 0 \\ 0 & \frac{1}{\sqrt{2}}\mathbb{1}_{N\times N} & -\frac{i}{\sqrt{2}}\mathbb{1}_{N\times N} \\ 0 & \frac{1}{\sqrt{2}}\mathbb{1}_{N\times N} & \frac{i}{\sqrt{2}}\mathbb{1}_{N\times N} \end{pmatrix}, \tag{13}$$

where $\mathbb{1}_{n\times n}$ and $\mathbb{1}_{N\times N}$ are the $n\times n$ and $N\times N$ identity matrices. The symbol † means Hermitian conjugation. A similarity transformation $\tilde{H}_{\text{eff}} = M^{\dagger}H_{\text{eff}}M$ of the effective Hamiltonian in Eq. (11) to the traveling-wave basis gives

$$\tilde{H}_{\text{eff}} = \tilde{H}^{(0)} + \tilde{H}^{(1)} = \begin{pmatrix} E_0 & 0 & 0 \\ 0 & E+F & 0 \\ 0 & 0 & E-F \end{pmatrix} + \begin{pmatrix} 0 & S_{\text{CCW}\to 0} & S_{\text{CW}\to 0} \\ S_{0\to\text{CCW}} & 0 & S_{\text{CW}\to\text{CCW}} \\ S_{0\to\text{CW}} & S_{\text{CCW}\to\text{CW}} & 0 \end{pmatrix} \tag{14}$$

with the complex $N\times N$ matrices

$$E = \frac{E_c + E_s}{2}, \quad F = i\frac{W - W^{\mathrm{T}}}{2}, \tag{15}$$

$$S_{\text{CW}\to\text{CCW}} = \frac{E_c - E_s}{2} - i\frac{W + W^{\mathrm{T}}}{2}, \tag{16}$$

$$S_{\text{CCW}\to\text{CW}} = \frac{E_c - E_s}{2} + i\frac{W + W^{\mathrm{T}}}{2}, \tag{17}$$

where $E^{\mathrm{T}} = E$, $F^{\mathrm{T}} = -F$, and with the $n\times N$ matrices

$$S_{\text{CCW}\to 0} = \frac{a + ib}{\sqrt{2}}, \quad S_{\text{CW}\to 0} = \frac{a - ib}{\sqrt{2}} \tag{18}$$

and the $N\times n$ matrices

$$S_{0\to\text{CCW}} = \frac{a^{\mathrm{T}} - ib^{\mathrm{T}}}{\sqrt{2}}, \quad S_{0\to\text{CW}} = \frac{a^{\mathrm{T}} + ib^{\mathrm{T}}}{\sqrt{2}}. \tag{19}$$

The matrix $E+F$ $(E-F)$ describes the forward scattering within the CCW (CW) components. The matrices $S_{\text{X}\to\text{Y}}$ belong to the scattering between different components ($m = 0$, CCW, CW).

In the following we assume that the scattering between counterpropagating traveling waves and the coupling of CW and CCW components to $m = 0$ components is weak. In this regime of weak backscattering we can consider $\tilde{H}^{(1)}$ as a perturbation to $\tilde{H}^{(0)}$ in Eq. (14). Note that this assumption is much less restrictive than assuming a weak perturbation of a rotationally invariant system. The $2N$ eigenstates of the unperturbed part $\tilde{H}^{(0)}$ without the $m = 0$ eigenstates are

$$v^{(0)}_{\text{CCW},j} = \begin{pmatrix} 0 \\ x^{(0)}_j \\ 0 \end{pmatrix}, \quad v^{(0)}_{\text{CW},j} = \begin{pmatrix} 0 \\ 0 \\ y^{(0)}_j \end{pmatrix}, \tag{20}$$

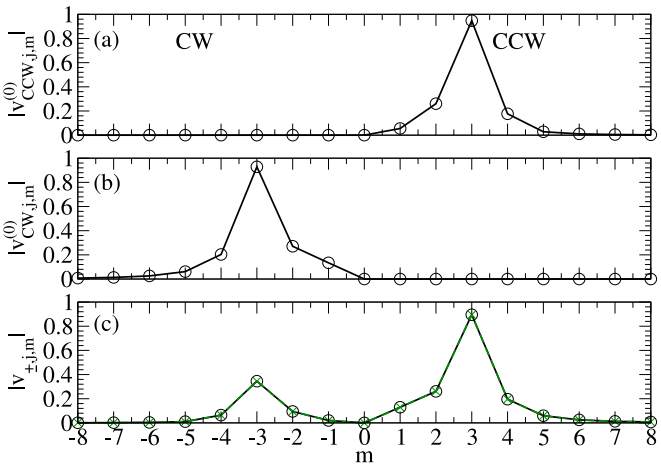

FIG. 6. (Color online) Components of the eigenvectors of $\tilde{H}^{(0)}$ (a) $v^{(0)}_{\mathrm{CCW},j}$ and (b) $v^{(0)}_{\mathrm{CW},j}$ (circles and solid lines) for the complex potential (2) corresponding to the eigenvectors of the full problem shown in Fig. 2. (c) The two resulting superpositions $v_{\pm,j}$ according to Eq. (32) (circles and black solid lines, and crosses and green dashed lines). The lines are guides to the eye.

where $v^{(0)}_{\mathrm{CCW},j}$ and $v^{(0)}_{\mathrm{CW},j}$ are $2N+n$-dimensional complex vectors and $x^{(0)}_j$ and $y^{(0)}_j$ are N-dimensional complex vectors. The latter fulfill the eigenvalue equations

$$(E+F)x^{(0)}_j = \Omega_{\mathrm{CCW},j}x^{(0)}_j, \tag{21}$$

$$(E-F)y^{(0)}_j = \Omega_{\mathrm{CW},j}y^{(0)}_j. \tag{22}$$

The vectors $x^{(0)}_j$ and $y^{(0)}_j$ are in general different but have the same eigenvalue $\Omega_j = \Omega_{\mathrm{CCW},j} = \Omega_{\mathrm{CW},j}$ because of $(E-F)^{\mathrm{T}} = (E+F)$ and the fact that the transposition of a square matrix does not change its eigenvalues. If the mirror-reflection-symmetry breaking is weak ($F \approx 0$) then $x^{(0)}_j \approx y^{(0)}_j$.

For illustration Figs. 6(a) and 6(b) show two eigenvectors $v^{(0)}_{\mathrm{CCW},j}$ and $v^{(0)}_{\mathrm{CW},j}$ for the example from the previous section. Clearly, these vectors are not just eigenstates of the kinetic part of the Hamiltonian but are influenced by the complex potential (2).

As $E+F$ is in general a non-Hermitian matrix, it is not guaranteed that the right eigenvectors $x^{(0)}_j$ are orthogonal to each other. To cure this deficiency we introduce the associated left eigenvectors,

$$(E+F)^{\dagger}\tilde{x}^{(0)}_j = \Omega^*_j\tilde{x}^{(0)}_j. \tag{23}$$

The set of eigenvectors $x^{(0)}_j$ and $\tilde{x}^{(0)}_i$ are assumed to form a biorthogonal basis with

$$\tilde{x}^{(0)\dagger}_i \cdot x^{(0)}_j = \delta_{ij}. \tag{24}$$

Moreover, we require the independent normalization condition $x^{(0)\dagger}_j \cdot x^{(0)}_j = 1$. The normalization for $\tilde{x}^{(0)\dagger}_j$ is then fixed by Eq. (24). It the same way we define a biorthogonal partner for $y^{(0)}_j$ by

$$(E-F)^{\dagger}\tilde{y}^{(0)}_j = \Omega^*_j\tilde{y}^{(0)}_j \tag{25}$$

with

$$\tilde{y}^{(0)\dagger}_i \cdot y^{(0)}_j = \delta_{ij} \tag{26}$$

and $y^{(0)\dagger}_j \cdot y^{(0)}_j = 1$. In the case of a non-Hermitian unperturbed Hamiltonian such biorthogonal bases have to be used for perturbation theory [32]. For given j the eigenvalue of $\tilde{H}^{(0)}$ is obviously twofold degenerate with the two eigenstates given by Eq. (20). We have therefore to employ degenerate perturbation theory using left and right eigenvectors; see for example [40]. In first order the perturbed eigenvalues and eigenstates can be computed by projecting the effective Hamiltonian $\tilde{H}_{\mathrm{eff}}$ onto the two-dimensional subspace spanned by the two eigenstates in Eq. (20). This gives the non-Hermitian 2×2 matrix

$$\tilde{H} = \begin{pmatrix} \Omega & A \\ B & \Omega \end{pmatrix} \tag{27}$$

with

$$A = \tilde{x}^{(0)\dagger}_j S_{\mathrm{CW}\to\mathrm{CCW}}\, y^{(0)}_j, \tag{28}$$

$$B = \tilde{y}^{(0)\dagger}_j S_{\mathrm{CCW}\to\mathrm{CW}}\, x^{(0)}_j, \tag{29}$$

where the dependence of Ω, A, and B on j is suppressed for notational convenience. The eigenvalues and (not normalized) eigenvectors of the effective Hamiltonian $\tilde{H}$ are given by

$$\Omega_{\pm} = \Omega \pm \sqrt{AB}, \tag{30}$$

$$\psi_{\pm} = \begin{pmatrix} \sqrt{A} \\ \pm\sqrt{B} \end{pmatrix}. \tag{31}$$

The corresponding eigenvectors in the original vector space are therefore

$$v_{\pm,j} = \begin{pmatrix} 0 \\ \sqrt{A}x^{(0)}_j \\ \pm\sqrt{B}y^{(0)}_j \end{pmatrix}. \tag{32}$$

Equations (27)–(32) constitute the central result of this paper. Using the eigenvectors (32) we can express the chirality [for 1D in Eq. (6)] as

$$\alpha = 1 - \frac{\min(|A|,|B|)}{\max(|A|,|B|)} \tag{33}$$

for both states and the overlap [for 1D in Eq. (7)] as

$$S = \frac{|v^{\dagger}_{+,j}\cdot v_{-,j}|}{\sqrt{v^{\dagger}_{+,j}\cdot v_{+,j}}\sqrt{v^{\dagger}_{-,j}\cdot v_{-,j}}} = \frac{||A|-|B||}{|A|+|B|}. \tag{34}$$

With the Eqs. (33) and (34) the relation between the overlap and the chirality in Eq. (8) can be easily derived.

To make the results clear, we again consider the saw-tooth potential from the previous section. Figure 6(c) shows two vectors $v_{\pm,j}$ for the potential (2) computed from Eqs. (27)–(32). A nice agreement with Fig. 2(a) can be observed. Moreover, our theory predicts the chirality $\alpha \approx 0.8572$ for both states and the overlap $S \approx 0.75$. This is in good

agreement with $\alpha \approx 0.8854$ and ≈ 0.8712, and $S \approx 0.7798$ from the full numerics having in mind that our treatment is based on first-order perturbation theory. The agreement improves considerably for higher eigenstates as the influence of the perturbation becomes effectively weaker. For instance, for the eigenvectors 12 and 13 we get $\alpha \approx 0.664$ and ≈ 0.6614, and $S \approx 0.4954$ from the full numerics and $\alpha \approx 0.6564$ for both states and the overlap $S \approx 0.4885$ from our theory. So, our theory gives quantitative correct values for the chirality and overlap. Moreover, the copropagation is self-evident from the structure of the vectors in Eq. (32).

It follows from Eqs. (16), (17), (28), and (29) that generically the backscattering between counterpropagating traveling waves is asymmetric, $|A| \neq |B|$. In the following special situations the backscattering is symmetric, $|A| = |B|$, in the presence of a mirror-reflection symmetry ($W = 0$) and for a closed system (W and $E_c - E_s$ are real-valued matrices). Clearly, only for symmetric backscattering the chirality α and the overlap S vanishes. For complete asymmetry in the backscattering ($A = 0$ with $B \neq 0$ or the other way around), we get $\alpha = 1$ and $S = 1$, i.e., full chirality and collinear eigenstates. The latter indicates an EP. In this case the eigenvalues (30) *and* eigenvectors (31) degenerate. From Eq. (32) it is clear that EPs of the 2×2 Hamiltonian (27) are also close to EPs of the full Hamiltonian (11) provided that the first-order perturbation theory describes the system accurately.

IV. CONCLUDING REMARKS

Our first-order perturbation theory shows that the interrelated phenomena nonorthogonality, chirality, and copropagation appear generically in open quantum and wave systems in which the backscattering between counterpropagating traveling waves is weak. Good quantitative agreement with a simple quantum system, a particle moving along a circle in a complex potential, is observed. The relation to exceptional points of the effective non-Hermitian Hamiltonian is explained.

The 2×2 non-Hermitian Hamiltonian (27) has been used previously as a phenomenological model to describe coupling of CCW and CW traveling waves in deformed microcavities [12,14]. In the case of the deformed disks it was unclear why the large set of different angular momentum components can be treated effectively as a two-state system (CW and CCW). Only for the special case of a dielectric circular disk perturbed by two nanoparticles, in which two angular momentum components dominate each state pair, was the Hamiltonian (27) rigorously derived in a two-state approximation [21]. Our theory here explains why the 2×2 non-Hermitian Hamiltonian (27) works so well also for the case in which many angular momentum components are involved.

Since the theory presented in this paper is very general, we expect to find the discussed phenomena not only in optical microdisk cavities and parity-time-symmetric quantum rings but also in other physical systems. As a final remark, we comment on the observability of these phenomena in experiments. The asymmetric backscattering could be directly detected in transmission and reflection measurements on a perturbed or deformed microdisk without any mirror-reflection symmetries coupled to two waveguides; see, e.g., [41]. The chirality could be observed in perturbed or deformed microdisk lasers since traveling waves can use the gain more efficiently [42]. The nonorthogonality of eigenstates in open quantum and wave systems can be observed indirectly by measuring changes of resonance widths resulting from Hermitian perturbations of the system [40].

ACKNOWLEDGMENTS

Fruitful discussions with H. Schomerus and D. V. Savin are acknowledged. This work was done in the framework of DFG Project No. WI1986/6-1.

[1] C. Keller, M. K. Oberthaler, R. Abfalterer, S. Bernet, J. Schmiedmayer, and A. Zeilinger, Phys. Rev. Lett. **79**, 3327 (1997).
[2] N. Syassen, D. M. Bauer, M. Lettner, T. Volz, D. Dietze1, J. J. García-Ripoll, J. I. Cirac, G. Rempe, and S. Dürr, Science **320**, 5881 (2008).
[3] P. Kaer, T. R. Nielsen, P. Lodahl, A. P. Jauho, and J. Mørk, Phys. Rev. Lett. **104**, 157401 (2010).
[4] C. E. Rüter, K. G. Makris, R. El-Ganainy, D. N. Christodoulides, M. Segev, and D. Kip, Nat. Phys. **6**, 192 (2010).
[5] E. Persson, I. Rotter, H.-J. Stöckmann, and M. Barth, Phys. Rev. Lett. **85**, 2478 (2000).
[6] C. Dembowski, H.-D. Gräf, H. L. Harney, A. Heine, W. D. Heiss, H. Rehfeld, and A. Richter, Phys. Rev. Lett. **86**, 787 (2001).
[7] K. J. Vahala, Nature (London) **424**, 839 (2003).
[8] G. Gamow, Z. Phys. **51**, 204 (1928).
[9] J. U. Nöckel and A. D. Stone, Nature (London) **385**, 45 (1997).
[10] C. Gmachl, F. Capasso, E. E. Narimanov, J. U. Nöckel, A. D. Stone, J. Faist, D. L. Sivco, and A. Y. Cho, Science **280**, 1556 (1998).
[11] H. E. Tureci, H. G. L. Schwefel, P. Jacqoud, and A. D. Stone, Prog. Opt. **47**, 75 (2005).
[12] J. Wiersig, S. W. Kim, and M. Hentschel, Phys. Rev. A **78**, 053809 (2008).
[13] S.-B. Lee, J. Yang, S. Moon, S.-Y. Lee, J.-B. Shim, S. W. Kim, J.-H. Lee, and K. An, Phys. Rev. Lett. **103**, 134101 (2009).
[14] J. Wiersig, A. Eberspächer, J.-B. Shim, J.-W. Ryu, S. Shinohara, M. Hentschel, and H. Schomerus, Phys. Rev. A **84**, 023845 (2011).
[15] T. Kato, *Perturbation Theory for Linear Operators* (Springer, New York, 1966).
[16] W. D. Heiss, Phys. Rev. E **61**, 929 (2000).
[17] M. V. Berry, Czech. J. Phys. **54**, 1039 (2004).
[18] W. D. Heiss and H. L. Harney, Eur. Phys. J. D **17**, 149 (2001).
[19] C. Dembowski, B. Dietz, H.-D. Gräf, H. L. Harney, A. Heine, W. D. Heiss, and A. Richter, Phys. Rev. Lett. **90**, 034101 (2003).
[20] J. Lekner, Pure Appl. Opt. **5**, 417 (1996).
[21] J. Wiersig, Phys. Rev. A **84**, 063828 (2011).
[22] D. D. Scott and Y. N. Joglekar, Phys. Rev. A **85**, 062105 (2012).
[23] I. Rotter, J. Phys. A **42**, 153001 (2009).

[24] H.-J. Stöckmann, E. Persson, Y.-H. Kim, M. Barth, U. Kuhl, and I. Rotter, Phys. Rev. E **65**, 066211 (2002).
[25] W. P. Reinhardt, Annu. Rev. Phys. Chem. **33**, 223 (1982).
[26] M. V. Berry and D. H. J. O'Dell, J. Phys. A: Math. Gen. **31**, 2093 (1998).
[27] S. Reitzenstein, S. Münch, P. Franeck, A. Löffler, S. Höfling, L. Worschech, A. Forchel, I. V. Ponomarev, and T. L. Reinecke, Phys. Rev. B **82**, 121306(R) (2010).
[28] G. E. Mitchell, A. Richter, and H. A. Weidenmüller, Rev. Mod. Phys. **82**, 2845 (2010).
[29] G. L. Celardo and L. Kaplan, Phys. Rev. B **79**, 155108 (2009).
[30] A. Lorke, S. Wimmer, B. Jager, J. P. Kotthaus, W. Wegschneider, and M. Bichler, Physica B **249-251**, 312 (1998).
[31] T. Salger, S. Kling, T. Hecking, C. Geckler, L. Morales-Molina, and M. Weitz, Science **326**, 124 (2009).
[32] M. M. Sternheim and J. F. Walker, Phys. Rev. C **6**, 114 (1972).
[33] W. B. Hodge, E. D. Welchman, and M. J. Rave, Eur. Phys. J. B **84**, 351 (2011).
[34] V. G. Baryshevskiĭ, V. I. Lyuboshitz, and M. I. Podgoretskiĭ, Sov. Phys. JETP **30**, 91 (1970).
[35] K. Petermann, IEEE J. Quantum Electron. **15**, 566 (1979).
[36] M. V. Berry, J. Mod. Opt. **50**, 63 (2003).
[37] H. Schomerus, Phys. Rev. A **79**, 061801(R) (2009).
[38] V. V. Sokolov, I. Rotter, D. V. Savin, and M. Müller, Phys. Rev. C **56**, 1044 (1997).
[39] S. Bennett, D. Nygren, H. Saal, J. Steinberger, and J. Sunderland, Phys. Rev. Lett. **19**, 997 (1967).
[40] Y. V. Fyodorov and D. V. Savin, Phys. Rev. Lett. **108**, 184101 (2012).
[41] A. Morand, Y. Zhang, B. Martin, K. P. Huy, D. Amans, P. Benech, J. Verbert, E. Hadji, and J.-M. Fédéli, Opt. Express **14**, 12814 (2006).
[42] A. E. Siegman, *Lasers* (University Science Books, Sausalito, CA, 1986).